Ther Adv Neurol Disord
2019, Vol. 12: 1–8
DOI: 10.1177/1756286419833295

Whole-brain magnetic resonance imaging of plaque burden and lenticulostriate arteries in patients with different types of stroke

Fang Wu, Qian Zhang, Kai Dong, Jiangang Duan, Xiaoxu Yang, Ye Wu, Ling Zhang, Debiao Li, Zhaoyang Fan and Qi Yang

Abstract

Background: Large-vessel atherosclerotic disease is an important pathogenesis of deep-perforator infarction (DPI). However, altered vessel walls of intracranial large arteries and distribution of small arteries in DPI are unclear because of the limited resolution of current imaging techniques. In this study the intracranial plaque burden and lenticulostriate artery (LSA) distribution in patients with recent DPI and non-DPI using whole-brain vessel-wall imaging (WB-VWI) were investigated.

Methods: A total of 44 patients with recent DPI (23 patients) or non-DPI (21 patients) due to intracranial atherosclerotic disease were prospectively enrolled. WB-VWI was performed in all the patients using a three-dimensional T1-weighted vessel-wall magnetic resonance technique. Hemispheres with DPI and non-DPI were considered as the DPI group and non-DPI group, respectively. Hemispheres without a history of stroke were the control group. The intracranial plaque burden was compared between the DPI and non-DPI groups. The number and length of visualized LSA branches among DPI, non-DPI, and control groups were also evaluated.

Results: A total of 77 hemispheres were analyzed (23 in the DPI group, 21 in the non-DPI group, and 33 in the control group). Plaque burden was lower ($p = 0.047$) in the DPI group ($82.0 \pm 45.9\,mm^3$) compared with the non-DPI group ($130.9 \pm 90.3\,mm^3$). There was a significant reduction ($p = 0.002$) in length of visualized LSA branches in the DPI group ($74.1 \pm 21.7\,mm$) compared with the control group ($104.6 \pm 33.3\,mm$).

Conclusions: WB-VWI enables the combination of vessel-wall and LSA imaging in one image setting, which can provide information about plaque burden and LSA distribution.

Keywords: high-resolution magnetic resonance imaging, intracranial atherosclerosis, lenticulostriate artery, stroke, vessel-wall imaging

Received: 28 September 2018; revised manuscript accepted: 11 December 2018.

Correspondence to:
Qi Yang
Department of Radiology, Xuanwu Hospital, Capital Medical University, Beijing, 100053, China
yangyangqiqi@gmail.com

Fang Wu
Department of Radiology, Xuanwu Hospital, Capital Medical University, Beijing, China

Qian Zhang
Kai Dong
Department of Neurology, Xuanwu Hospital, Capital Medical University, Beijing, China

Jiangang Duan
Department of Neurosurgery, Xuanwu Hospital, Capital Medical University, Beijing, China

Xiaoxu Yang
Ye Wu
Department of Radiology, Xuanwu Hospital, Capital Medical University, Beijing, China

Ling Zhang
Department of Radiology, Beijing Luhe Hospital, Capital Medical University, Beijing, China

Debiao Li
Zhaoyang Fan
Biomedical Imaging Research Institute, Cedars-Sinai Medical Center, Los Angeles, CA, USA, and Departments of Medicine and Bioengineering, University of California, Los Angeles, CA, USA

Introduction

The deep perforating branches from the middle cerebral artery (MCA) feed the basal ganglia and internal capsule by the lenticulostriate arteries (LSAs).[1] Deep-perforator infarction (DPI) is considered to be caused by large-artery atherothrombosis that blocks the orifice of the perforating artery, small-vessel disease, or cardioembolism.[2,3] The differentiation between large-artery atherothrombosis and small-vessel disease is clinically important, since different mechanisms causing DPI necessitate distinct clinical managements. Systemic anti-atherosclerotic medication, such as statins, may be effective in patients with large-artery atherothrombosis, whereas management of blood pressure with antiplatelet agents may be useful in patients with small-vessel disease.[4,5] Thus, a robust imaging

technique that can depict both the vessel-wall structure of large intracranial arteries and the patency of perforating arteries is valuable in the exploration of stroke pathogenesis.

Computed tomography angiography (CTA) and magnetic resonance angiography (MRA) have been used for imaging of intracranial arteries for decades. A previous study has investigated the visualization of LSA branches by CTA and compared LSA changes caused by ageing and hypertension.[6] However, the CT imaging used in this study had limited resolution, which may not be sufficient for small LSA branches. Intracranial MR vessel-wall imaging (VWI) has appeared as a high sensitivity modality for detecting intracranial atherosclerotic plaques.[7,8] Several studies have shown that MCA plaques can be detected in 40–63.2% of patients with DPI by two-dimensional VWI, suggesting that proximal occlusion of a perforating artery by a parent artery plaque is an important cause of DPI.[9,10]

Recently, three-dimensional (3D) VWI techniques have provided an opportunity for a global assessment of intracranial atherosclerotic plaques and total intracranial plaque burden.[11,12] A previous study has proved that extracted vascular trees of LSA branches on VWI were in good agreement with MRA at 7 tesla.[13] Thus, the aim of our study was to investigate the intracranial plaque burden and LSA status in patients with recent DPI and non-DPI using whole-brain vessel-wall imaging (WB-VWI) at 3 tesla.

Methods

Patients

Between May 2016 and November 2017, patients with acute stroke admitted to the Department of Neurology were prospectively recruited with the following inclusion criteria: (a) DPI or non-DPI identified in the MCA territory using diffusion-weighted imaging (DWI) performed within 72 h of symptom onset; (b) stenosis or irregularity on the relevant MCA or intracranial internal carotid artery (ICA), as confirmed by MRA, CTA, or digital subtraction angiography. Exclusion criteria were: (a) previous history of ipsilateral stroke or transient ischemic attacks; (b) history of ipsilateral MCA or intracranial ICA occlusion; (c) co-existent 50% or more stenosis or unstable plaques of the ipsilateral extracranial carotid artery detected by ultrasound; (d) evidence of cardioembolism. All of the enrolled patients underwent WB-VWI, time-of-flight MRA (TOF-MRA), and DWI within 2 weeks of symptom onset. Patients who had any of the following features were also excluded from the study: (a) any new lesions detected on repeated DWI; (b) non-atherosclerotic vasculopathy that may predispose to stroke (e.g. vasculitis, Moyamoya disease, or dissection), which was diagnosed by two experienced neurologists with clinical risk factors, blood tests, and all imaging tests (including lumen imaging and precontrast and postcontrast WB-VWI). Informed consent was obtained from all participants, and all protocols were approved by the Institutional Review Board.

Routine imaging evaluation

Routine MR images (T1-, T2-weighted, fluid-attenuated inversion recovery, and DWI) were interpreted by one reader and the infarction pattern was categorized into two groups as follows: (a) DPI defined as hyperintense areas on DWI localized in the striatocapsular area, including the putamen, globus pallidus, internal capsule, and caudate head (Figure 1(a)); (b) non-DPI when infarct areas are localized in the MCA territory, but outside the striatocapsular area (Figure 1(b)). Any hemispheres without a history of stroke were considered as controls.

WB-VWI protocols

All patients underwent WB-VWI, TOF-MRA, and DWI with a 3-tesla system (MAGNETOM Verio, Siemens, Erlangen, Germany) and a standard 32-channel head coil. WB-VWI was performed based on inversion recovery-prepared SPACE with the following parameters: TR/TE = 900/15 ms; field of view = 170 × 170 mm^2; 240 slices with slice thickness of 0.53 mm; voxel size = 0.53 × 0.53 × 0.53 mm^3; scan time = 8 min. Postcontrast WB-VWI was performed 5 min after the injection of single-dose (0.1 mmol per kg of body weight) gadolinium-based contrast agent (Magnevist, Schering, Berlin, Germany). Imaging parameters for TOF-MRA were: TR/TE = 22/4 ms; field of view = 170 × 170 mm^2; 155 slices with slice thickness of 0.7 mm; voxel size = 0.5 × 0.5 × 0.7 mm^3; scan time = 6 min. DWI was performed: TR/TE of 5500/90 ms; field of view 240 × 240 mm^2; 20 slices with slice thickness of 5 mm; voxel size = 1.8 × 1.8 × 5 mm^3; 2 *b* values of 0 and 1000 s/mm^2; scan time of 40 s.

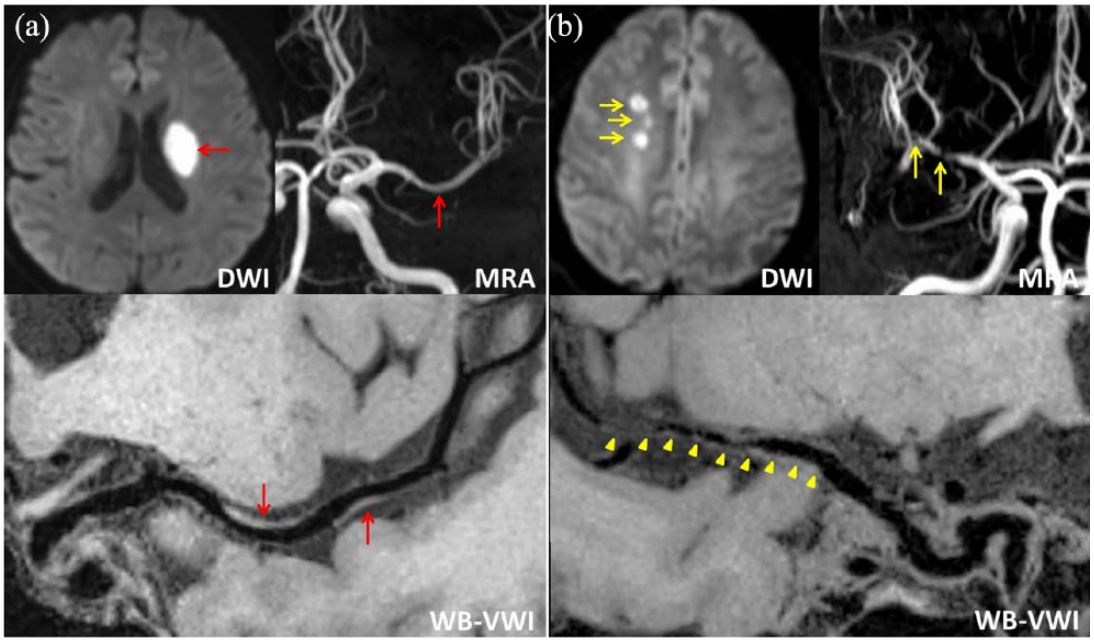

Figure 1. Representative cases of deep-perforator infarction (DPI) (a) and non-DPI (b). (a) Diffusion-weighted imaging (DWI) with a high signal intensity lesion (red arrow) in the left basal ganglia, magnetic resonance angiography (MRA) with mild stenosis in the left middle cerebral artery (MCA) (red arrow), whole-brain vessel-wall imaging (WB-VWI) revealing focal plaques (red arrows) in the left MCA. (b) DWI showing multiple high signal intensity lesions (yellow arrow) in the right centrum ovale, multiple severe stenosis of the right MCA (yellow arrows) by MRA, WB-VWI with diffuse plaques in the right MCA (yellow arrowheads).

WB-VWI image evaluation

Since in the present study, we mainly focused on the association of plaque burden, LSA branches, and stroke, only precontrast images were included for the evaluation. Evaluation of WB-VWI was conducted by a neuroradiologist (Wu) who was blinded to the clinical details and routine images of patients by commercial software (VA, Vessel Analysis, Beijing, China). A subgroup of hemispheres with infarction ($n = 20$) was included to study the reproducibility of measurements. A second reader (Yang) performed quantification to assess inter-observer agreement and reader 1 (Wu) requantified the measurements 2 months after the first reading session to assess intra-observer agreement.

Image quality was evaluated by means of a three-point scale (0: not visualized; 1: poor; 2: good and excellent). Images that were not able to delineate the LSA branches or vessel-wall contour were graded as not visualized. Images that did not allow clear and commendable visualization of the LSA branches or vessel-wall structure were graded as poor. Images with optimal quality that allowed the best visualization of vessel-wall structure and LSA branches were graded as good and excellent. Only patients with good and excellent quality images were included in our analyses.

Plaque burden was defined as the total volume of all atherosclerotic plaques (thickening of the vessel wall using its adjacent proximal, distal, or contralateral vessel segment as a reference) on ipsilateral MCA (M1 ~ M3 segment) and intracranial ICA, identified on WB-VWI. The total plaque burden of each subject was operationalized by manually dyeing the plaques on precontrast 3D multiplanar reformation images and summed volumes of the plaques (mm^3) were automatically calculated.

LSA images were generated using coronal minimum intensity projection with 10–15 mm thickness on precontrast WB-VWI. The number and total length of visualized LSA branches on the symptomatic side of each subject and the control side were measured. LSA branches 5 mm or more in length were included for analysis.[14] When an artery branched within 5 mm of the origin of the MCA, each branch was counted separately.[1]

Table 1. Patient characteristics of the two groups.

	DPI ($n = 23$)	Non-DPI ($n = 21$)	p value
Male gender, no. (%)	19 (82.6)	15 (71.4)	0.481
Age (mean ± SD, years)	55.5 ± 12.4	50.2 ± 10.4	0.132
Hypertension, no. (%)	17 (73.9)	17 (81.0)	0.724
Diabetes mellitus, no. (%)	6 (26.1)	6 (28.6)	0.853
Hyperlipidemia, no. (%)	9 (39.1)	8 (38.1)	0.944
Current smoking, no. (%)	13 (56.5)	11 (52.4)	0.783
Onset to WB-VWI time (mean ± SD, days)	8.9 ± 3.9	10.8 ± 2.8	0.073

DPI, deep-perforator infarction; SD, standard deviation; WB-VWI, whole-brain vessel-wall imaging.

When an artery branched at a more distal site, only the longest branch was measured.[14]

Statistical analysis

All continuous variables were expressed as means ± standard deviation and categorical variables were summarized as count (percentage). Clinical characteristics between DPI and non-DPI patients were compared using the Mann–Whitney *U* test for continuous variables and the chi-square test for categorical variables. Differences in plaque burden between DPI and non-DPI groups were assessed using the Mann–Whitney *U* test. The number and length of visualized LSA branches among DPI, non-DPI, and control groups were calculated by the Kruskal–Wallis test and *post hoc* pairwise comparisons. Intra- and inter-reader agreement in measurements was assessed by intraclass correlation coefficients (ICC) with a one-way random effect for intra-observer continuous variables and a two-way random effect for inter-observer continuous variables. A p value of less than 0.05 indicated statistical significance. All statistical analyzes were performed by using commercial software (SPSS 22.0, IBM).

Results

Patient characteristics

Among the 59 patients who were recruited, 15 patients were excluded due to low quality (grade 0 or 1) WB-VWI images. A total of 44 patients (23 with DPI and 21 with non-DPI) were finally included for analyzes. The median interval between symptom onset and WB-VWI was 9.8 ± 3.5 days (ranging from 3 days to 14 days). Patient demographics and main clinical characteristics are presented in Table 1. No statistically significant differences were found.

Measurement reliability

A good intra-observer reliability for plaque burden, branch number, and branch length was found, with ICC (95% confidence interval) of 0.92 (0.82–0.97), 0.77 (0.51–0.90), and 0.89 (0.75–0.96). Inter-observer reproducibility for the above measurements was also strong, with ICC (95% confidence interval) of 0.88 (0.73–0.95), 0.75 (0.48–0.89), and 0.81 (0.58–0.92), respectively.

Plaque burden and LSA distribution

A total of 77 hemispheres were analyzed, including 23 in the DPI group, 21 in the non-DPI group, and 33 in the control group. Plaque burden was lower ($p = 0.047$) in the DPI group (82.0 ± 45.9 mm^3) compared with the non-DPI group (130.9 ± 90.3 mm^3).

The average length of visualized LSA branches was 74.1 ± 21.7 mm in the DPI group, 89.3 ± 31.8 mm in the non-DPI group, and 104.6 ± 33.3 mm in the controls. There was a significant reduction in length in the DPI group ($p = 0.002$) compared with the control group. However, no differences were found between the DPI group and non-DPI group (p =

Table 2. Plaque burden and number/length of LSA branches.

	DPI	Non-DPI	Controls	*p* value			
					DPI *versus* controls	Non-DPI *versus* controls	DPI *versus* non-DPI
Plaque burden (mean ± SD, mm^3)	82.0 ± 45.9	130.9 ± 90.3	—	0.047	—	—	—
Branch number (mean ± SD, no.)	3.3 ± 1.0	4.1 ± 1.0	4.2 ± 1.1	0.436	—	—	—
Branch length (mean ± SD, mm)	74.1 ± 21.7	89.3 ± 31.8	104.6 ± 33.3	0.003	0.002	0.495	0.207

DPI, deep-perforator infarction; LSA, lenticulostriate artery; SD, standard deviation.

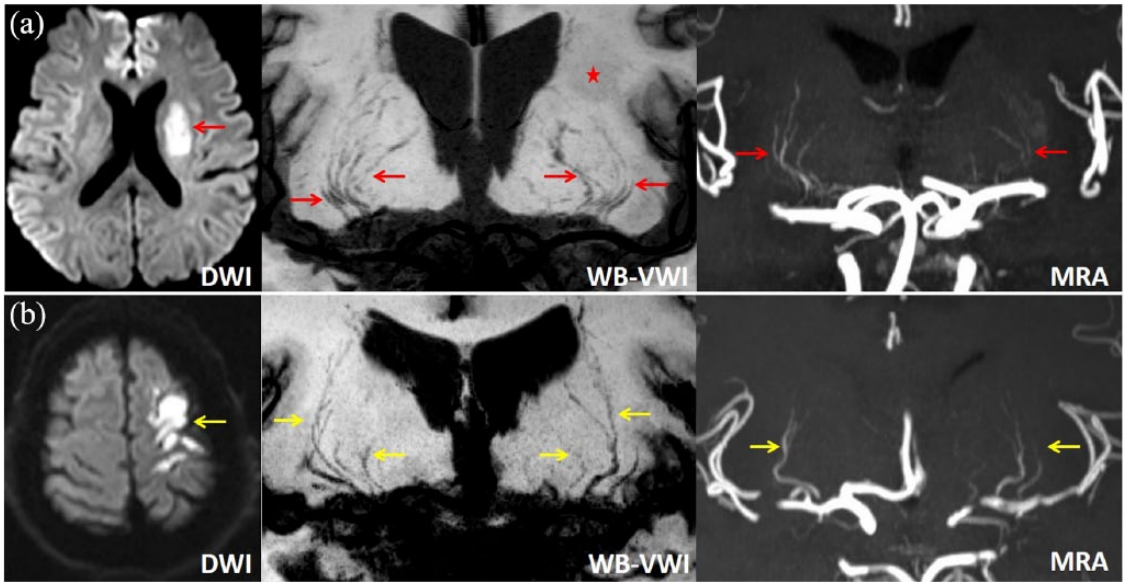

Figure 2. Representative cases of DPI (a) and non-DPI (b). (a) DWI with a high signal intensity lesion (red arrow) in the left basal ganglia, WB-VWI and MRA showing pruning of the left LSA branches compared with the right normal side (red arrows), and WB-VWI revealing the left infarction with slightly low signal intensity (asterisk). (b) DWI with multiple high signal intensity lesions (yellow arrow) in the left cortico-subcortical area, WB-VWI and MRA revealing almost symmetrical LSA branches of the ipsilateral left and the contralateral right hemispheres (yellow arrows).

0.207), as well as the non-DPI group *versus* the control group ($p = 0.495$).

The average number of visualized LSA branches was 3.3 ± 1.0, 4.1 ± 1.0, and 4.2 ± 1.1 for the DPI, non-DPI, and control groups, respectively. The number of LSA branches did not differ among these three groups.

Details of plaque burden and LSA features are described in Table 2 and Figures 1–3.

Discussion

In this study, we found that the DPI group had a lower plaque burden compared with the non-DPI group. In addition, we also found a significant reduction in the length of LSA branches in the DPI group compared with the control group, whereas the number of LSA branches showed no difference among the DPI group, non-DPI group, and control group. To the best of our knowledge, this is the first study using WB-VWI to explore the intracranial

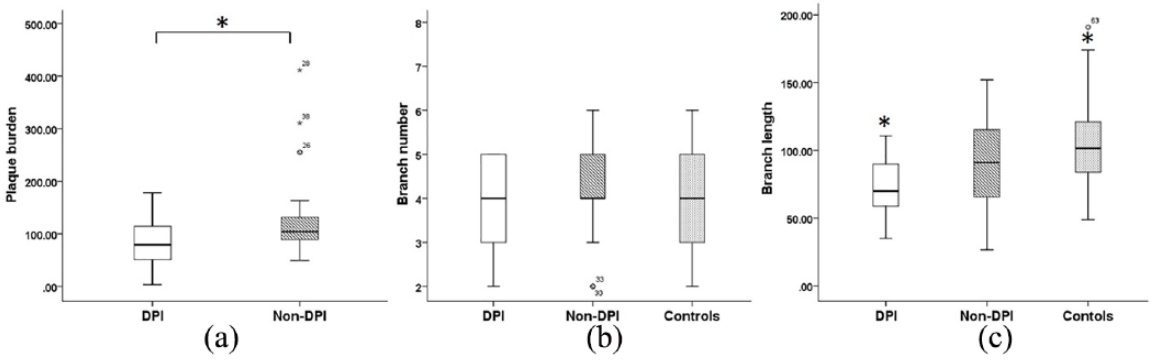

Figure 3. Plaque burden (a), branch number (b), and branch length (c) of DPI, non-DPI, and the controls. Non-DPI group has a higher plaque burden compared with DPI group (in (a) asterisk indicates $p = 0.047$). There was a significant reduction in branch length in the DPI group compared with the controls (in (c) asterisk indicates $p = 0.002$).

plaque burden and LSA characteristics in different types of stroke.

Several studies have demonstrated that flow-sensitive black-blood MRA based on 3D gradient-echo sequence can be specifically used to visualize LSAs.[14–16] The relationship between decreased LSA visualization and infarction has been reported.[16] WB-VWI is capable of depicting LSA branches due to the adequate black-blood effect of the SPACE acquisition within the small LSAs and well-suppressed perivascular fluid by the use of inversion preparation.[17,18] However, visualization of LSAs needs high quality VWI images with less motion artifacts. In the present study, nearly 25% of patients with acute stroke were excluded due to poor image quality induced by motion artifact. Thus, a motion-free WB-VWI technique is needed to better visualize LSAs. We found that the DPI group had a significant reduction in length of LSA branches compared with the control group, which was in line with Okuchi and colleagues' study.[16] In the DPI group, occlusion at the orifice of the LSA branches caused by a parent artery plaque may result in a decrease of blood flow and thrombosis in the distal part of these small arteries. Then, the disappearance of a hypointense area in the lumen brings about the decreased visualization of LSA branches. In addition, decrease of cerebral blood inflow in patients with severe stenosis of the proximal large arteries may also influence the visualization of small branches. Further study is needed to investigate the association between LSA features and various degrees of stenosis.

In our study, the number of LSA branches showed no difference among the three groups. This result suggests that the number of LSA branches can remain unchanged in DPI, which may be partly explained by the compensatory mechanism due to the opening of more small vessels or incomplete occlusion of the perforating arteries. This result disagrees with Okuchi and colleagues' study reporting a significant reduction in the number of LSA branches in patients with a stroke at the basal ganglia and/or its vicinity.[16] This divergence may be because patients with chronic infarction were mainly included in their study, while recent stroke patients were analyzed in our work.

Plaque burden, as a global evaluating indicator, may provide supplementary information on the extent of atherosclerosis beyond luminal stenosis degree and plaque morphology. However, the association of how plaque burden relates with different stroke subtypes is still unclear. Though automatic or semi-automatic segmentation in the measurement of plaque burden has been used in carotid atherosclerotic diseases,[19,20] these methods remain difficult to use in intracranial arteries due to the smaller vessel diameter. In our study, reliable analysis software was used to acquire the plaque volume by manually segmenting and automatically calculating. We found that the DPI group had a lower plaque burden compared with the non-DPI group ($p = 0.047$), however the p value was very close to 0.05 indicating weak difference.

Combined imaging of vessel wall and LSA could provide valuable insights for understanding the mechanism and pathophysiology of DPI. By using this powerful technique in microvascular imaging, this study offers additional evidence for directly proving the relationship between infarction and microvascular damage. The potential of

noninvasive screening and detection of LSA abnormalities would contribute to identifying patients at risk and facilitate preventive therapeutic interventions.

The present study has several limitations. First, a p value of 0.047 was found for the difference of plaque burden between the DPI and non DPI groups. The relatively small sample size of this study included possible selection bias, further large sample data need to be fully investigated to verify this result and explore the relationship between LSA distribution and the size of the infarction. Second, in this preliminary study, we only discuss the plaque burden and LSA changes in patients with DPI with intracranial atherosclerotic disease. In future, we should also include patients with DPI without large atherosclerotic disease and explore the LSA changes in DPI with different pathogenesis. Third, there were no other imaging examinations that could provide a contrast in the visualization of LSA branches, since LSA distribution was compared between WB-VWI at 3 tesla and MRA at 7 tesla in our previous study.

In conclusion, the DPI group showed a significant reduction in the length of visualized LSA branches compared with the controls. WB-VWI enables the combination of vessel-wall and LSA imaging in one image setting, which can provide information about plaque burden and the degeneration of perforating arteries.

Funding

This work was supported in part by the National Key Research and Development Program of China (2016YFC1301702 and 2017YFC1307903), Beijing Natural Science Foundation (L172043), and the National Science Foundation of China (NSFC 91749127).

Conflict of interest statement

The authors declare no conflicts of interest in preparing this article.

References

1. Marinkovic S, Gibo H, Milisavljevic M, *et al.* Anatomic and clinical correlations of the lenticulostriate arteries. *Clin Anat* 2001; 14: 190–195.
2. Bang OY, Heo JH, Kim JY, *et al.* Middle cerebral artery stenosis is a major clinical determinant in striatocapsular small, deep infarction. *Arch Neurol* 2002; 59: 259–263.
3. Kang DW, Chalela JA, Ezzeddine MA, *et al.* Association of ischemic lesion patterns on early diffusion-weighted imaging with toast stroke subtypes. *Arch Neurol* 2003; 60: 1730–1734.
4. Bang OY. Intracranial atherosclerosis: current understanding and perspectives. *J Stroke* 2014; 16: 27–35.
5. Furie KL, Kasner SE, Adams RJ, *et al.*; American Heart Association Stroke Council, Council on Cardiovascular Nursing, Council on Clinical Cardiology and Interdisciplinary Council on Quality of Care and Outcomes Research. Guidelines for the prevention of stroke in patients with stroke or transient ischemic attack: a guideline for healthcare professionals from the American heart association/American stroke association. *Stroke* 2011; 42: 227–276.
6. Gotoh K, Okada T, Satogami N, *et al.* Evaluation of CT angiography for visualisation of the lenticulostriate artery: difference between normotensive and hypertensive patients. *Br J Radiol* 2012; 85: e1004–e1008.
7. Mandell DM, Mossa-Basha M, Qiao Y, *et al.*; Vessel Wall Imaging Study Group of the American Society of Neuroradiology. Intracranial vessel wall MRI: principles and expert consensus recommendations of the American Society of Neuroradiology. *AJNR Am J Neuroradiol* 2017; 38: 218–229.
8. Qiao Y, Guallar E, Suri FK, *et al.* MR imaging measures of intracranial atherosclerosis in a population-based study. *Radiology* 2016; 280: 860–868.
9. Chung JW, Kim BJ, Sohn CH, *et al.* Branch atheromatous plaque: a major cause of lacunar infarction (high-resolution MRI study). *Cerebrovasc Dis Extra* 2012; 2: 36–44.
10. Yoon Y, Lee DH, Kang DW, *et al.* Single subcortical infarction and atherosclerotic plaques in the middle cerebral artery: high-resolution magnetic resonance imaging findings. *Stroke* 2013; 44: 2462–2467.
11. van der Kolk AG, Zwanenburg JJ, Brundel M, *et al.* Intracranial vessel wall imaging at 7.0-t MRI. *Stroke* 2011; 42: 2478–2484.
12. Qiao Y, Steinman DA, Qin Q, *et al.* Intracranial arterial wall imaging using three-dimensional high isotropic resolution black blood MRI at 3.0 tesla. *J Magn Reson Imaging* 2011; 34: 22–30.
13. Zhang Z, Fan Z, Kong Q, *et al.* Visualization of the lenticulostriate arteries at 3T using black-blood

T1-weighted intracranial vessel wall imaging: comparison with 7T TOF-MRA. *Eur Radiol* 2018; 29: 1452–1459.

14. Gotoh K, Okada T, Miki Y, *et al*. Visualization of the lenticulostriate artery with flow-sensitive black-blood acquisition in comparison with time-of-flight MR angiography. *J Magn Reson Imaging* 2009; 29: 65–69.
15. Okuchi S, Okada T, Fujimoto K, *et al*. Visualization of lenticulostriate arteries at 3T: optimization of slice-selective off-resonance sinc pulse-prepared TOF-MRA and its comparison with flow-sensitive black-blood MRA. *Acad Radiol* 2014; 21: 812–816.
16. Okuchi S, Okada T, Ihara M, *et al*. Visualization of lenticulostriate arteries by flow-sensitive black-blood MR angiography on a 1.5 T MRI system: a comparative study between subjects with and without stroke. *AJNR Am J Neuroradiol* 2013; 34: 780–784.
17. Fan Z, Yang Q, Deng Z, *et al*. Whole-brain intracranial vessel wall imaging at 3 tesla using cerebrospinal fluid-attenuated T1-weighted 3D turbo spin echo. *Magn Reson Med* 2017; 77: 1142–1150.
18. Yang Q, Deng Z, Bi X, *et al*. Whole-brain vessel wall MRI: a parameter tune-up solution to improve the scan efficiency of three-dimensional variable flip-angle turbo spin-echo. *J Magn Reson Imaging* 2017; 46: 751–757.
19. Selwaness M, Hameeteman R, Van't Klooster R, *et al*. Determinants of carotid atherosclerotic plaque burden in a stroke-free population. *Atherosclerosis* 2016; 255: 186–192.
20. van't Klooster R, de Koning PJ, Dehnavi RA, *et al*. Automatic lumen and outer wall segmentation of the carotid artery using deformable three-dimensional models in MR angiography and vessel wall images. *J Magn Reson Imaging* 2012; 35: 156–165.